Neuropsychopharmacology (2009) 34, 624–633

www.neuropsychopharmacology.org

Tiagabine Increases [^{11}C]flumazenil Binding in Cortical Brain Regions in Healthy Control Subjects

W Gordon Frankle*[,1,2], Raymond Y Cho[1], Rajesh Narendran[1,2], N Scott Mason[2], Shivangi Vora[1], Maralee Litschge[1], Julie C Price[2], David A Lewis[1,3] and Chester A Mathis[2]

[1]Department of Psychiatry, University of Pittsburgh, Pittsburgh, PA, USA; [2]Department of Radiology, University of Pittsburgh, Pittsburgh, PA, USA; [3]Department of Neuroscience, University of Pittsburgh, Pittsburgh, PA, USA

Accumulating evidence indicates that synchronization of cortical neuronal activity at γ-band frequencies is important for various types of perceptual and cognitive processes and that GABA-A receptor-mediated transmission is required for the induction of these network oscillations. In turn, the abnormalities in GABA transmission postulated to play a role in psychiatric conditions such as schizophrenia might contribute to the cognitive deficits seen in this illness. We measured the ability to increase GABA in eight healthy subjects by comparing the binding of [^{11}C]flumazenil, a positron emission tomography (PET) radiotracer specific for the benzodiazepine (BDZ) site, at baseline and in the presence of an acute elevation in GABA levels through the blockade of the GABA membrane transporter (GAT1). Preclinical work suggests that increased GABA levels enhance the affinity of GABA-A receptors for BDZ ligands (termed 'GABA shift'). Theoretically, such an increase in the affinity of GABA-A receptors should be detected as an increase in the binding of a GABA-A BDZ-receptor site-specific PET radioligand. GAT1 blockade resulted in significant increases in mean (± SD) [^{11}C]flumazenil-binding potential (BP_{ND}) over baseline in brain regions representing the major functional domains of the cerebral cortex: association cortex + 15.2 ± 20.2% ($p = 0.05$), sensory cortex + 13.5 ± 15.5% ($p = 0.03$) and limbic (medial temporal lobe, MTL) + 16.4 ± 20.2% ($p = 0.03$). The increase in [^{11}C]flumazenil-BP_{ND} was not accounted for by differences in the plasma-free fraction (f_P; paired t-test $p = 0.24$) or changes in the nonspecific binding (pons V_T, $p = 0.73$). Moreover, the ability to increase GABA strongly predicted ($r = 0.85$, $p = 0.015$) the ability to entrain cortical networks, measured through EEG γ synchrony during a cognitive control task in these same subjects. Although additional studies are necessary to further validate this technique, these data provide preliminary evidence of the ability to measure *in vivo*, with PET, acute fluctuations in extracellular GABA levels and provide the first *in vivo* documentation of a relationship between GABA neurotransmission and EEG γ-band power in humans.
Neuropsychopharmacology (2009) **34,** 624–633; doi:10.1038/npp.2008.104; published online 9 July 2008

Keywords: GABA; PET; [^{11}C]flumazenil; GABA shift; γ-band; oscillations

INTRODUCTION

Accumulating evidence indicates that synchronization of cortical neuronal activity at γ-band frequencies is important for various types of perceptual (Sanes and Donoghue, 1993; Tiitinen *et al*, 1993; Lutzenberger *et al*, 1995) and cognitive processes (Miltner *et al*, 1999; Howard *et al*, 2003). In a recent electroencephalogram (EEG) study, we found that increases in context maintenance demands were associated with the increases in induced γ activity over prefrontal cortical areas for healthy controls (Cho *et al*, 2006). Experimental models (Van Vreeswijk *et al*, 1994; Bartos *et al*, 2007) as well as preclinical studies (Hajos *et al*, 2004; Mann *et al*, 2005; Fuchs *et al*, 2007) suggest that GABA-A receptor-mediated transmission is required for the induction of network oscillations. However, to date, there is no evidence linking GABA transmission with γ-band oscillations in humans. Over the last few years, several groups have demonstrated that receptor imaging techniques (single photon emission computerized tomography, SPECT, or positron emission tomography, PET) can be used, not only to measure receptor parameters, but also to detect acute changes in the concentration of endogenous neurotransmitters in the vicinity of their receptors (for review see Laruelle, 2000). These studies have yielded important insights into the pathophysiology of mental illnesses such as schizophrenia and substance abuse (Laruelle *et al*, 1996; Breier *et al*, 1997; Volkow *et al*, 1997; Abi-Dargham *et al*, 2000; Martinez *et al*, 2005, 2007). However, such studies have thus far been largely limited to the dopamine system due to a lack of suitable radiotracers and methodology for other neurotransmitter systems.

*Correspondence: Dr WG Frankle, Departments of Psychiatry and Radiology, University of Pittsburgh, Western Psychiatric Institute and Clinic, 3811 O'Hara Street, Pittsburgh, PA 15213, USA,
Tel: +412 246 5829, Fax: +412 586 9040,
E-mail: franklewg@upmc.edu
Received 16 April 2008; revised 23 May 2008; accepted 27 May 2008

The aim of this study was to determine the feasibility of developing a technique for measuring changes in synaptic GABA levels with PET across brain regions representing the major functional domains of the cerebral cortex (association, sensory, and limbic). Such a technique could have widespread utility in the study of mental illness as GABA abnormalities have been implicated in a variety of psychiatric conditions. For example, a large body of postmortem and preclinical work has revealed abnormalities in markers of GABA function in schizophrenia (for review see Lewis *et al*, 2005). These abnormalities have been most consistently observed in the dorsolateral prefrontal cortex (DLPFC), but altered expression levels of GABA-related gene products in schizophrenia have been found across cortical areas, including the anterior cingulate, motor, visual, and auditory cortices (Impagnatiello *et al*, 1998; Woo *et al*, 2004; Konopaske *et al*, 2006; Hashimoto *et al*, in press) suggesting that alterations in GABA neurotransmission could contribute to the cognitive, affective, sensory, and motor signs and symptoms of this disorder. GABA abnormalities are also hypothesized to play a role in disorders such as alcohol dependence (Krystal *et al*, 2006), anxiety (Nemeroff, 2003), and mood disorders (Brambilla *et al*, 2003). However, to date, there is no direct, *in vivo* evidence that GABA transmission is altered in any of these illnesses.

Using a novel PET brain-imaging paradigm, we measured the *in vivo* binding of the benzodiazepine (BDZ) site-specific radiotracer [^{11}C]flumazenil (Persson *et al*, 1985) at baseline and in the context of elevated GABA levels induced through blockade of the GABA membrane transporter (GAT1) with tiagabine (Gabitril®). Preclinical work suggests that increased GABA levels enhance the affinity of GABA-A receptors for BDZ ligands through a conformational change (termed the 'GABA- shift') (Tallman *et al*, 1978; Braestrup *et al*, 1982; Miller *et al*, 1988). Theoretically, such an increase in the affinity of GABA−A receptors should be detected as an increase in the binding of a GABA-A BDZ-receptor site-specific PET radioligand. Eight healthy subjects underwent two [^{11}C]flumazenil PET scans on the same day, baseline, and 30 min after administration of oral tiagabine. Tiagabine inhibits the reuptake of GABA by selective GAT1 blockade resulting in acute increases in extracellular GABA levels (Fink-Jensen *et al*, 1992). Our hypothesis was that cortical [^{11}C]flumazenil binding, measured through PET, would be increased in the context of elevated brain GABA levels resulting from GAT1 blockade. We then explored the relationship between this *in vivo* measurement of GABA transmission and cortical synchrony in the γ-band range (30–80 Hz), as phasic GABA-A receptor-mediated neurotransmission is postulated to be required for induction of network oscillations in this range (Whittington and Traub, 2003).

MATERIALS AND METHODS

Human Subjects

The study was approved by the Institutional Review Board of the University of Pittsburgh Medical Center. Eight healthy volunteers participated in this study (age 29 ± 10 years, range: 20–50, with these and subsequent values given as mean ± SD, four men and four women). All scans were performed within the 2-month period between 25 June 2007 and 24 August 2007. The absence of pregnancy, medical, neurological, and psychiatric history (including alcohol and drug abuse) was assessed by history, review of systems, physical examination, routine blood tests including pregnancy test, urine toxicology, and EKG. Subjects provided written informed consent after receiving an explanation of the study.

PET Protocol

All subjects were studied twice with [^{11}C]flumazenil on the same day. On the study day, an arterial catheter was inserted in the radial artery, after completion of the Allen test and infiltration of the skin with lidocaine, for blood sampling and a venous catheter was inserted in a forearm vein for radiotracer injection. First, a baseline PET scan was performed. The baseline scan was followed by oral administration of tiagabine 16 mg with the second, on-medication, PET scan beginning 30 min post-tiagabine administration. This dose of tiagabine is expected to increase extracellular GABA by 50% over baseline for several hours (During *et al*, 1992).

The scanning protocol was identical for each scan. PET imaging was performed with the ECAT EXACT HR+ (Siemens/CTI, Knoxville, TN). A 10 min transmission scan was obtained before each radiotracer injection for attenuation correction of the emission data. [^{11}C]flumazenil was produced through a modification of published procedures (Halldin *et al*, 1988). Twenty mCi or less of high-specific activity (1379 ± 393 Ci/mmoles) [^{11}C]flumazenil was injected i.v. over 30 s. Emission data were collected in the 3D mode for 90 min as 19 successive frames of increasing duration (4×15 s, 3×1 min, 3×2 min, 2×5 min, and 7×10 min). Subjects were allowed to rest outside of the camera for 30–60 min between the two injections. Subjects remained in the Montefiore University Hospital Clinical and Translational Research Center overnight after the PET scans to monitor for any side effects of tiagabine administration. Adverse effects observed in this study included sedation (mild-to-moderate) and ataxia (mild) and resolved completely within 4 h of the scan.

Input Function Measurement

Following radiotracer injection, arterial samples were collected manually approximately every 6 s for the first 2 min and thereafter at longer intervals. A total of 35 samples were obtained per scan. Following centrifugation (2 min at 12 500 r.p.m., Spectrafuge 16 M), plasma was collected in 200 l aliquots and activities were counted in a γ counter (Packard Biosciences).

To determine the plasma activity representing unmetabolized parent compound, seven samples (collected at 2, 5, 15, 30, 45, 75, and 90 min) were further processed through aqueous/organic extraction (Barre *et al*, 1991) to measure the fractional concentrations of hydrophilic metabolites and unchanged (lipophilic) [^{11}C]flumazenil. The seven measured unmetabolized fractions were fitted to the sum of one exponential plus a constant and this function was used to interpolate values between the measurements.

The input function was calculated as the product of total counts and interpolated unmetabolized fraction at each time point. The measured input function values were fitted to a sum of three exponentials from the time of peak plasma activity and the fitted values were used as the input to the kinetic analysis. The clearance of the parent compound (l/h) was calculated as the ratio of the injected dose to the area under the curve of the input function (Abi-Dargham *et al*, 1994).

For the determination of the plasma-free fraction (f_P), triplicate aliquots of plasma collected before injection were mixed with the radiotracer, pipetted into ultrafiltration units (Amicon Centrifree; Bedford, MA) and centrifuged at room temperature (30 min at 6000 r.p.m.). At the end of centrifugation, the plasma and ultrafiltrate activities were counted (Packard Biosciences), and f_P was calculated as the ratio of activity in the ultrafiltrate to total activity (Price *et al*, 1993). Triplicate aliquots of saline solution mixed with the radiotracer were also processed to determine the filter retention of the free tracer.

MRI Acquisition and Segmentation Procedures

To provide an anatomical framework for analysis of the PET data, MRI scans were obtained using a 1.5 T GE Medical Systems (Milwaukee, WI) Signa Scanner. A 3D spoiled gradient-recalled sequence was acquired in the coronal plane using parameters that were optimized for maximal contrast among gray matter, white matter, and CSF. The scalp and calvarium were removed from the SPGR MR images, to facilitate MR/PET coregistration, using a manual in-house stripping technique. MRI segmentation was performed using the FAST automated segmentation tool (Zhang *et al*, 2001) implemented in the FMRIB Software Library (v4.0, Smith *et al*, 2004).

Image Analysis

PET data were reconstructed using filtered backprojection (Fourier rebinning/2D backprojection, 3 mm Hann filter) and corrected for photon attenuation (^{68}Ge/^{68}Ga rods), scatter (Watson, 2000), and radioactive decay. Reconstructed image files were then processed with the image analysis software MEDx (Sensor Systems Inc., Sterling, VA) with the PET-MR image alignment performed using the SPM2 package (www.fil.ion.ucl.ac.uk/spm). PET data were inspected for subject motion and interframe motion was corrected using the realign procedure within SPM2, if necessary.

Regions of interest (ROIs) were drawn on each individual's MRI according to the criteria derived from brain atlases (Talairach and Tournoux, 1988; Duvernoy, 1991) and applied to the coregistered dynamic PET data to generate regional time–activity curves. Three functionally-based cortical ROIs were obtained as weighted averages of component ROIs: association cortex (dorsolateral prefrontal, orbital frontal, medial prefrontal, and anterior cingulate), Sensory cortex (parietal and occipital), and the limbic MTL (amygdala (AMY), hippocampus (HIP), entorhinal cortex (ENT), and parahippocampal gyrus (PHG)). The pons was used as the region of reference as activity in this region represents predominantly nonspecific binding (Koeppe *et al*, 1991; Abadie *et al*, 1992; Price *et al*, 1993).

For the neocortical regions, 'large' regions were first drawn to delineate the boundaries of the ROIs. Within these regions, only the voxels classified as gray matter were used to measure the activity distribution. Sampled volumes of the neocortical regions ($n = 6$) were as follows: DLPFC(22 352 ± 2133 mm^3), orbitofrontal cortex (OFC, 13 149 ± 5207 mm^3), medial prefrontal cortex (MPFC, 4562 ± 1033 mm^3), anterior cingulate cortex (ACC, 5435 ± 620 mm^3), parietal cortex (PC, 63 998 ± 8444 mm^3), and occipital cortex (OC, 53 302 ± 7486 mm^3).

Because of the mixture of gray and white matter in the structures of the MTL, the segmentation-based approach was not used for the ROIs component, and the boundaries of these regions were identified by anatomical criteria. These regions ($n = 4$) included AMY (2803 ± 719 mm^3), HIP (3958 ± 630 mm^3), ENT (1314 ± 336 mm^3), and PHG (5876 ± 858 mm^3).

For bilateral regions, right and left values were averaged. The contribution of plasma total activity to the regional activity was calculated assuming a 5% blood volume in ROIs (Mintun *et al*, 1984) and tissue activities were calculated as the total regional activities minus the plasma contribution.

Derivation of Distribution Volumes

We denote here the outcome variables using the recently issued consensus nomenclature for *in vivo* imaging of reversibly binding radioligands (Innis *et al*, 2007). Derivation of [^{11}C]flumazenil regional tissue distribution volume (V_T, ml/*g*) was performed with kinetic modeling using the arterial input function and an unconstrained two tissue compartment model (2TC model). V_T, which is equal to the ratio of tissue to plasma parent activity at equilibrium, was derived as $K_1/k_2(1 + k_3/k_4)$, where K_1 (ml/*g*/min) and k_2 (per min) are the unidirectional fractional rate constants governing the transfer into and out of the brain, respectively, and k_3 (per min) and k_4 (per min) are the unidirectional fractional rate constants governing the association and dissociation of [^{11}C]flumazenil to and from the BZD site, respectively (Koeppe *et al*, 1991; Laruelle *et al*, 1994; Innis *et al*, 2007). Kinetic parameters were derived by nonlinear regression using a Levenberg–Marquart least-squares minimization procedure (Levenberg, 1944) implemented in MATLAB (The Math Works Inc., South Natick, MA), as described previously(Laruelle *et al*, 1994). Given the unequal sampling over time (increasing frame acquisition time from the beginning to the end of the study), the least-squares minimization procedure was weighted by the frame acquisition time.

Derivation of BDZ Receptor Parameters

Derivation of BDZ parameters was based upon the following assumptions: (1) because of the low density of BDZ in the pons (Abadie *et al*, 1992; Price *et al*, 1993), pons V_T was assumed to be representative of equilibrium nonspecific binding, V_{ND}; (2) the nonspecific binding did not vary significantly between regions.

Two measures of BDZ receptor availability were derived using pons V_T to estimate the nondisplaceable distribution volume, V_{ND}.

The [^{11}C]flumazenil binding potential (BP_{ND}) relative to the total plasma concentration of [^{11}C]flumazenil (BP_P, ml/*g*) was derived as the difference between V_T in the ROI and V_{ND}. The relationship between BP_P and BDZ receptor parameters is given by $BP_P = f_P{*}B_{max}/K_D$, where B_{max} is GABA-A BDZ-receptor density, $1/K_D$ is the *in vivo* affinity of [^{11}C]flumazenil for the GABA-A BDZ-receptor and f_P is the fraction of the radiotracer unbound to protein in the plasma.

The [^{11}C]flumazenil-BP_{ND} relative to V_{ND} (BP_{ND}, unitless) was derived using the arterial input as BP_P/V_{ND} as well as using the simplified reference tissue method (SRTM, Lammertsma and Hume, 1996) with the pons as the reference region. SRTM utilizes assumptions 1 and 2, above, to infer a functional relationship between a reference region (pons) and an ROI. This method has been demonstrated to provide estimates of [^{11}C]flumazenil $BP_{ND,}$ which are highly correlated with arterial input methods (Klumpers *et al*, 2007). The relationship between BP_{ND} and BDZ receptor parameters is given by $BP_{ND} = f_{ND}{*}B_{max}/K_D$, where B_{max} is GABA-A BDZ-receptor density, $1/K_D$ is the *in vivo* affinity of [^{11}C]flumazenil for the GABA-A BDZ-receptor and f_{ND} is the fraction of the radiotracer unbound to protein in the brain.

Electrophysiology and Cognitive Task

In all subjects, the PET scans were performed before the electrophysiology study. The half-life of tiagabine ranges from 7–9 h; however, to minimize any potential interaction between the drug and the EEG measurements at least 5 days (43 ± 73) separated the tiagabine administration and the EEG.

The preparing to overcome prepotency (POP) task is a cued stimulus–response reversal paradigm that requires increases in cognitive control to overcome prepotent response tendencies (Cho *et al*, 2006). Trials proceeded in the following order: cue (a green or red square; 500 ms); delay period (1000 ms); probe (a white arrow pointing left or right; 1000 ms); and a variable intertrial interval (1000–2000 ms). Cues indicated conditions requiring either low (green square) or high (red square) degrees of cognitive control. Over the delay period, subjects were required to maintain the trial type information and prepare for a response to the upcoming probe. For low-control trials, subjects were required to respond in the direction of the arrow that followed (eg, for a right-pointing arrow, press the right button); for the high-control trials, responses were required in the opposite direction (eg, for a right-pointing arrow, press the left button). To reinforce the prepotency of the cue-–probe mappings of the low-control trials, thereby increasing the control requirements during the high-control trials, 70% of the trials were low control and the remaining 30% were high control. Trial types were interleaved in pseudorandom order, with eight blocks of 42 trials each.

During the POP task, EEG data were acquired using a 129 Ag-AgCl coated carbon fiber electrode Geodesic Sensor Net (EGI, Eugene, OR) with a sampling frequency of 250 Hz. Data were filtered on-line with a 0.1–100 Hz band pass hardware filter. Electrode impedances were kept below 50 kΩ. All channels were referenced to Cz. Data were filtered off-line using an 8–100 Hz bandpass, 60 Hz notch Butterworth Filter (time constant: 0.0199 s, slope: 12 dB/oct). Epochs were defined as −500 to +1700 ms relative to the cue onset. Blink artifacts were removed with ICA-based detection and correction methods. Error trials and remaining epochs containing artifacts were excluded (amplitude range exceeding 200 μV within a segment; or greater than 20 channels having 60 μV deviations between consecutive samples). Segments identified by these criteria were visually inspected before the final rejection. Average segment counts for the high- and low-control conditions were 220 and 80, respectively. Data were rereferenced to average reference (Bertrand *et al*, 1985).

Time-frequency analyses were carried out using Brain Vision Analyzer (Brain Products GmbH, Munich, Germany). The data were transformed using complex Morlet wavelet transforms, defined by $mo(x) = c \cdot \exp(-x^2/2) \cdot \exp(i\omega_0 x)$, with $c = 7$, using 40 frequency steps spanning 8–100 Hz. Wavelet transformed data were baseline corrected to a −300 to −50 ms precue interval.

EEG analysis involved identifying frontal areas of peak induced (ie not time locked to stimulus) γ activity differences between the high- and low-control conditions, with a focus on the delay period (500–1500 ms relative to the cue onset) during which induced-frontal γ activity has been shown to modulate in accordance with the cognitive control demands (Cho *et al*, 2006). Activity from one representative electrode from each of the left and right frontal areas, respectively, was averaged to derive a spatially averaged measure for comparison to the PET data. The peak activity was in the γ sub-band with central frequency 46 Hz, and electrode locations E8 and E24 (approximately AF8 and AF3, respectively, in the 10–10 system). This procedure resulted in one summary measure of frontal γ activity for each subject, which were then compared to the individual measurements of tiagabine-induced increase in [^{11}C]flumazenil binding by PET. Note that an experimenter blind to the PET data performed the determinations of these EEG measures of frontal γ.

Statistical Analysis

The between-scan comparisons were assessed with a paired, two-tailed *t*-test with a significance level of 0.05. As this was a preliminary study designed to determine the feasibility of moving forward with this methodology, we were more concerned with type II errors (not recognizing a significant effect) than with type I errors (false rejection of the null hypothesis). As such, baseline and post-tiagabine K_1, V_T and BP_{ND} for the three functional cortical regions and V_{ND} (pons V_T) were compared using a two-tailed, paired *t*-test, with an uncorrected probability value of 0.05 selected as the significance level. For the analysis of the tiagabine-induced change in V_T, $BP_{P,}$ and BP_{ND} in the component ROIs ($n = 10$), a univariate repeated-measure analysis of variance (RM ANOVA) with brain regions as the within-scan factor and condition (baseline or post-tiagabine) as the between-scan factor was used. Paired *t*-tests were performed, when appropriate, to determine which regions accounted for the significant effects observed in the RM ANOVA. The

relationship between the PET scan outcome measures and the measurement of γ-band power were analyzed with the Pearson product moment correlation coefficient after confirming normal distribution of the data using the Kolmogorov–Smirnov test.

RESULTS

PET Scan Parameters

No difference was observed in the injected dose, specific activity or injected mass between the baseline and post-tiagabine scan (Table 1). Tiagabine administration did not affect the plasma clearance of [^{11}C]flumazenil, [^{11}C]flumazenil plasma-free fraction (f_P), or the free and nonspecific binding in the brain (V_{ND}) measured as the distribution volume (V_T) of [^{11}C]flumazenil in the pons (Table 1). As $f_{ND} = f_P/V_{ND}$ (Innis *et al*, 2007), the lack of effect on f_P or V_{ND} supports the validity of using BP_{ND} as an outcome measure.

Regional Distribution Volumes and BZD Receptor Availability

After the administration of tiagabine, V_T increased significantly in the large cortical regions (these and subsequent values noted as mean ± SD, *p*-values for two-tailed, paired *t*-test unless otherwise stated); association cortex 6.2 ± 0.6 ml/*g* *vs* 7.1 ± 1.0 ml/*g* ($p = 0.05$), sensory cortex 6.4 ± 0.6 ml/*g* *vs* 7.3 ± 0.9 ml/*g* ($p = 0.03$), and limbic MTL 5.0 ± 0.4 ml/*g* *vs* 5.6 ± 0.6 ml/*g* ($p = 0.05$). Examination of V_T across the ROIs component revealed a significant regional effect (RM ANOVA $F = 274.3$, d.f. = 10, 5, $p < 0.0001$), no region by condition interaction (RM ANOVA $F = 0.55$, d.f. = 10, 5, $p = 0.65$), and a significant difference across the conditions (RM ANOVA $F = 5.30$, d.f. = 1, 14, $p = 0.04$). Increases in all regions were seen post-tiagabine (Figure 1), which were significant in the MPFC ($p = 0.04$), PC ($p = 0.04$), OC ($p = 0.04$), AMY ($p = 0.04$), ENT ($p = 0.05$), and PHG ($p = 0.04$).

Table 1 Demographic and Scan Data

Parameter	Baseline	Post-tiagabine	*p*
N	8	8	—
Age	29.1 ± 9.6	—	—
Gender	4M/4F	—	—
Ethnicity	1AA/6C/1AS	—	—
Tiagabine dose (mg/kg)	—	0.21 ± 0.05	—
Injected dose (mCi)	17.2 ± 3.8	17.5 ± 2.4	0.65
SA (Ci/mmoles)	1441 ± 287	1318 ± 490	0.44
Injected mass (μg)	3.7 ± 0.9	4.5 ± 1.4	0.21
Free fraction (f_P, %)	58.1 ± 6	61.4 ± 7	0.24
Clearance (l/h)	45 ± 13	94 ± 73	0.11
Pons V_T (or V_{ND} ml/*g*)	1.0 ± 0.2	1.0 ± 0.2	0.73

AA, African–American, AS, Asian, C, Caucasian, SA, specific activity. Significance level given is for a paired, two-tailed *t*-test.

Similarly, tiagabine-induced increases in [^{11}C]flumazenil-BP_{ND} were seen across all regions, whether BP was computed relative to the nondisplaceable reference (BP_{ND}) or plasma (BP_P). Unlike V_T, the BP measures are adjusted for nonspecific radioactivity and are therefore more reflective of specific binding.

BP_P increased in the cortical regions, nonsignificantly in the association cortex ($p = 0.06$) and significantly in the sensory cortex ($p = 0.03$) and MTL ($p = 0.05$) after the administration of tiagabine (Table 2). On a regionwise basis, tiagabine resulted in a significant increase in BP_P over baseline values (RM ANOVA, $F = 6.3$, d.f. = 1, 14, $p = 0.03$). Post hoc paired t-tests revealed that this increase was significant in the MPFC ($p = 0.05$), PC ($p = 0.04$), OC ($p = 0.04$), AMY ($p = 0.05$), and the PHG ($p = 0.05$).

Tiagabine resulted in the increases in BP_{ND} across all regions (Table 2 and Figure 2). BP_{ND} values were similar whether derived through arterial input method or SRTM; given this, in Table 2, the percent change in BP_{ND} (ΔBP_{ND}), the Cohen's effect size (*d*), and the region-by-region *p* value for a paired *t*-test are listed only for BP_{ND} derived through SRTM. Although the RM ANOVA was not significant ($p = 0.25$ for arterial method, $p = 0.29$ for SRTM), examining BP_{ND} in the component ROIs on a region-by-region basis revealed trend-level or significant comparisons (Table 2).

Electroencephalogram (EEG)-Induced γ-Band Oscillations

To test our hypothesis that individuals with greater capacity to increase GABA levels (a 'GABA reserve') would exhibit enhanced frontal γ-band oscillatory activity in the context of a task that taps cognitive control processes, seven individuals (four male and three female, age 30 ± 10 years) who participated in the PET study also underwent EEG

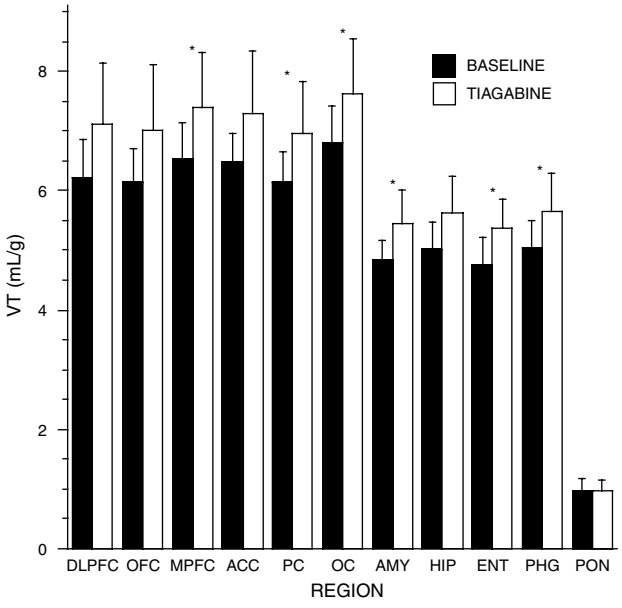

Figure 1 [^{11}C]flumazenil regional distribution volumes (V_T) at baseline (black bars) and post-tiagabine (white bars). Values are mean ± SD ($n = 8$). Regions abbreviated as in text. *Two-tailed, paired *t*-test $p < 0.05$.

Table 2 Tiagabine-Induced Change in [^{11}C]flumazenil BP_P and BP_{ND} in Control Subjects

Subdivision - Component ROIs	Baseline BP_P	Post-tiagabine BP_P	Baseline BP_{ND}	Post-tiagabine BP_{ND}	Baseline BP_{ND} (SRTM)	Post-tiagabine BP_{ND} (SRTM)	ΔBP_{ND}[a] (%)	d[a]	p[a]
Association cortex	5.3 ± 0.6	6.1 ± 0.9	5.7 ± 1.3	6.3 ± 0.7	5.8 ± 1.4	6.6 ± 1.2	15.2 ± 20.2	0.60	0.05
DLPFC	5.3 ± 0.7	6.1 ± 0.9	5.7 ± 1.3	6.3 ± 0.7	5.8 ± 1.4	6.6 ± 1.2	16.3 ± 20.8	0.63	0.04
Orbital frontal cortex	5.2 ± 0.6	6.0 ± 0.9	5.5 ± 1.2	6.2 ± 0.7	5.7 ± 1.3	6.4 ± 1.3	14.9 ± 20.8	0.59	0.07
MPFC	5.5 ± 0.7	6.4 ± 0.8	6.0 ± 1.4	6.7 ± 1.0	6.1 ± 1.4	6.8 ± 1.2	13.6 ± 18.4	0.56	0.06
Anterior cingulate cortex	5.5 ± 0.5	6.3 ± 0.9	5.9 ± 1.3	6.5 ± 0.6	6.0 ± 1.4	6.7 ± 1.3	14.1 ± 20.2	0.56	0.08
Sensory cortex	5.4 ± 0.6	6.3 ± 0.7	5.8 ± 1.2	6.5 ± 0.6	6.0 ± 1.3	6.7 ± 1.3	13.5 ± 15.5	0.59	0.03
Parietal cortex	5.2 ± 0.6	6.0 ± 0.7	5.6 ± 1.2	6.2 ± 0.6	5.7 ± 1.3	6.4 ± 1.3	13.9 ± 16.2	0.58	0.03
-Occipital cortex	5.8 ± 0.6	6.6 ± 0.8	6.2 ± 1.3	6.9 ± 0.7	6.4 ± 1.4	7.1 ± 1.3	13.0 ± 14.9	0.58	0.04
Medial temporal lobe	4.0 ± 0.5	4.6 ± 0.4	4.3 ± 1.1	4.8 ± 0.6	4.4 ± 1.1	5.0 ± 1.0	16.4 ± 20.2	0.60	0.03
Amygdala	3.9 ± 0.4	4.5 ± 0.4	4.2 ± 1.0	4.6 ± 0.5	4.2 ± 1.1	4.8 ± 0.8	17.1 ± 19.9	0.66	0.02
Hippocampus	4.0 ± 0.6	4.7 ± 0.5	4.3 ± 1.1	4.8 ± 0.6	4.4 ± 1.1	5.1 ± 1.0	17.7 ± 23.2	0.65	0.05
Entorhinal cortex	3.8 ± 0.6	4.4 ± 0.4	4.1 ± 1.2	4.6 ± 0.7	4.2 ± 1.3	4.8 ± 1.2	17.6 ± 23.3	0.47	0.03
Parahippocampus	4.1 ± 0.5	4.7 ± 0.5	4.4 ± 1.1	4.8 ± 0.7	4.5 ± 1.1	5.0 ± 1.1	15.4 ± 18.9	0.56	0.03

DLPF, dorsolateral prefrontal cortex; MPFC, medial prefrontal cortex; ROIs, regions of interest; SRTM, simplified reference tissue method. Values are Mean ± SD, in healthy controls ($n = 8$); p is the significance level of the difference between the baseline and post-tiagabine scans (paired t-test); d is the Cohen's effect size of this difference.
[a]Values of ΔBP_{ND}, d and p for BP_{ND} derived through SRTM.

measurement of frontal lobe γ-band oscillations during the POP task (Cho *et al*, 2006). Frontal cortical γ-band power was measured in each individual as the average of left (E24) and right (E8) electrodes during the delay period; these electrodes showed the highest γ-band activity in the group average, as determined by a rater blind to the PET data. Figure 3, panel a, shows a strong correlation ($r = 0.85$, $p = 0.015$) between γ-band power and the ability to increase extracellular GABA levels in the association cortex. Examining the component regions separately revealed similarly strong correlations (eg, DLPFC $r = 0.84$, $p = 0.019$). This relationship was not driven by a correlation between γ-band power and [^{11}C]flumazenil BP_{ND} in the association cortex at baseline (Figure 3, panel b) or post-tiagabine (Figure 3, panel c). No relationship was observed between behavioral performance on the POP task and γ-band power or change in [^{11}C]flumazenil binding as all individuals performed at a high level on the task (error rates 6.4 ± 8.5% for the high-control trials).

DISCUSSION

The results of this study are consistent with the hypothesis that the acute increases in extracellular cortical GABA can be detected as an increase in the binding of the BDZ site-specific radiotracer, [^{11}C]flumazenil. The principle underlying this hypothesis is the 'GABA shift'—the enhancement in BDZ-receptor affinity for BDZ site substrates resulting from the increased GABA (Tallman *et al*, 1978; Braestrup *et al*, 1982). It is widely accepted that BDZs potentiate the effects of GABA at the GABA-A receptor and the reverse is true, increased GABA levels potentiate the binding of BDZs to the GABA-A receptor in a dose-dependent manner (Tallman *et al*, 1978). However, some *in vitro* studies exploring this phenomenon with BDZ antagonists (including flumazenil, previously known as Ro15-1788) indicate that it is specific to agonist drugs (Mohler and Richards, 1981) and not all *in vitro* studies were able to demonstrate the GABA shift, even with BDZ agonists (Rosenberg and Chiu, 1979). Two preclinical studies have examined the effects of increasing GABA and GABAergic drugs on flumazenil binding in intact animals and both found results consistent with our findings. The first (Koe *et al*, 1987) demonstrated enhanced [^{3}H]flumazenil-binding *in vivo* when mice were treated with either progabide (a GABA analog and agonist at the GABA-A receptor) or valproate, which increases brain GABA levels (Johannessen, 2000). The second (Miller *et al*, 1988) measured the effects of three GABAergic drugs, aminooxyacetic acid (inhibitor of GABA transaminase, the enzyme that metabolizes GABA), γ-vinyl GABA (GVG, irreversible GABA transaminase inhibitor), and valproate on [^{3}H]flumazenil binding. All three drugs resulted in the acute increases in cortical GABA concentrations; with GVG treatment, GABA levels returned to baseline by 12 h. Specific binding of [^{3}H]flumazenil increased acutely across all brain regions, with all three drugs, with no change in nonspecific binding. No change in [^{3}H]flumazenil binding was observed with GVG once GABA levels returned to baseline.

Several groups have examined the *in vivo* susceptibility of [^{11}C]flumazenil binding to changes in GABA using PET in humans. Studies conducted at the University of Pittsburgh and in Finland detected an increase in [^{11}C]flumazenil binding following isoflurane (+16 to +28%, depending on brain region), sevoflurane (+20%), and propofol (+8%) (Gyulai *et al*, 2001; Salmi *et al*, 2004). These volatile anesthetics, presumably by enhancing GABA binding to GABA-A receptors, resulted in a dose-dependent increase in

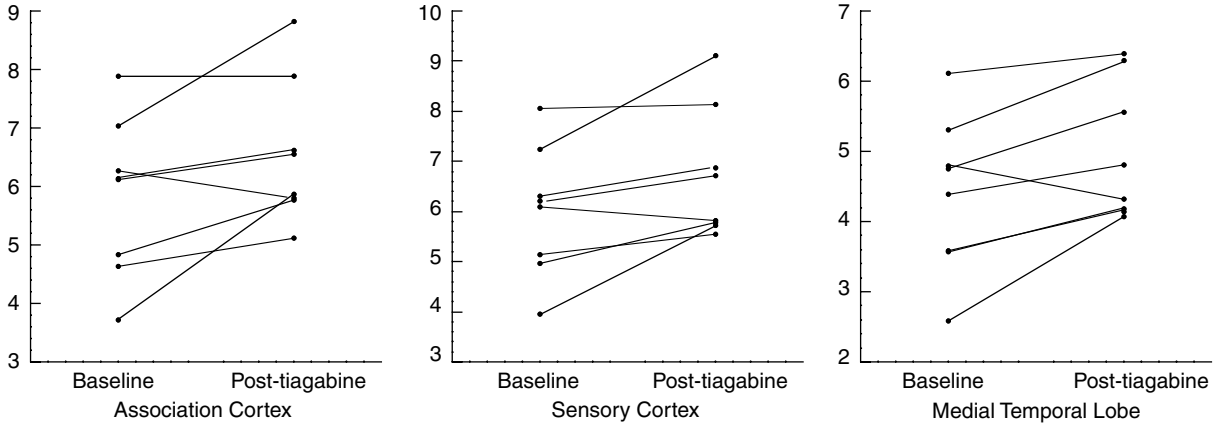

Figure 2 [11C]flumazenil-binding potential (BP_{ND}) derived through SRTM in eight healthy control individuals at baseline and 30 min after receiving tiagabine 16 mg p.o. Notably, one individual displayed decreased [11C]flumazenil binding across all regions.

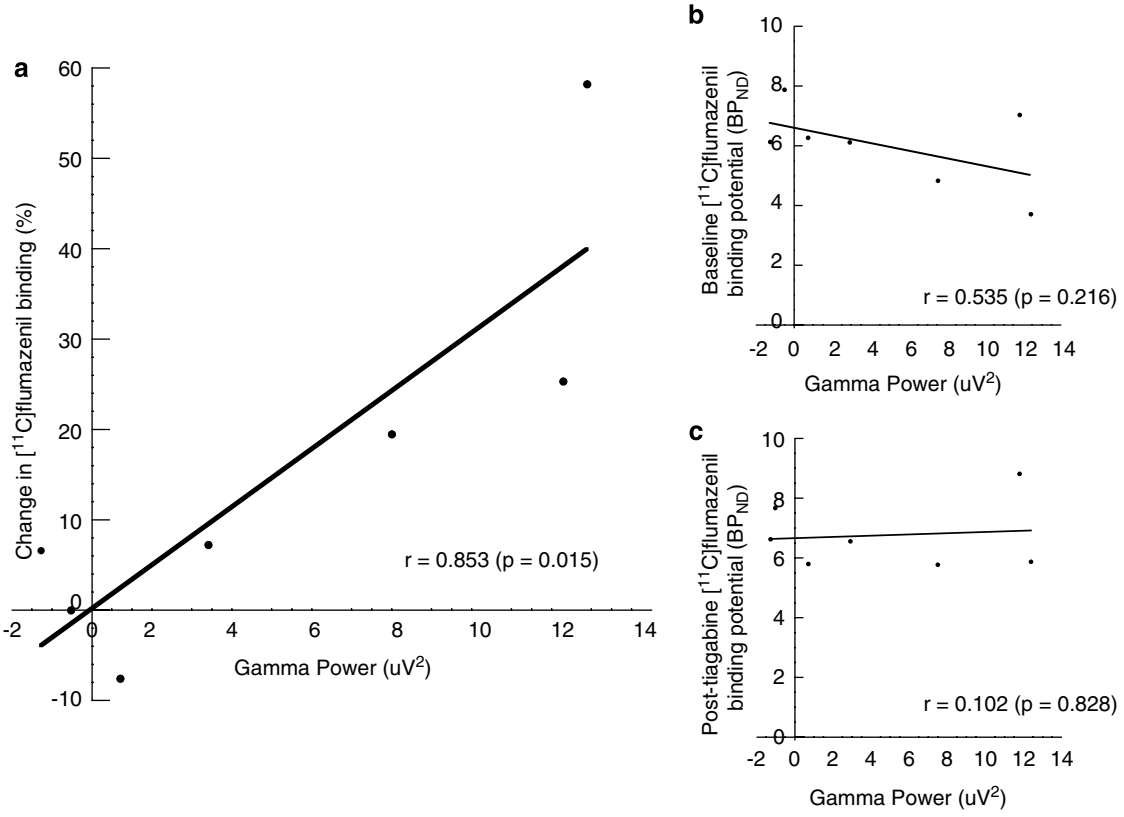

Figure 3 The ability to increase GABA levels in the association cortex, measured as the change in [11C]flumazenil binding in response to GAT1 blockade, strongly predicts ($r = 0.85$, $p = 0.015$) the ability to entrain cortical networks, measured through EEG γ oscillations (a). This relationship was not driven by a correlation between γ-band power and [11C]flumazenil-binding potential in the association cortex at baseline (b) or post-tiagabine (c).

[11C]flumazenil binding. Increases in [11C]flumazenil binding were not observed following subanesthetic doses of ketamine (an NMDA antagonist) suggesting that this effect is specific to anesthetics that interact with the GABA system (Salmi *et al*, 2005).

To our knowledge, only one previous study has been conducted in humans with a nonanesthetic compound, the irreversible GABA transaminase inhibitor GVG (Weber *et al*, 1999). In this study, GVG caused a trend level increase in [11C]flumazenil binding (the authors report increases in binding ranging from 0.6 to 22.1%, $p > 0.09$). While this is within the range of normal variability, in no subject did post-GVG [11C]flumazenil binding decrease (as one would expect if the change was entirely due to normal variability).

Using a somewhat similar paradigm to the one used in this study, several groups have attempted to measure changes in the apparent affinity of BDZ agonists using [11C]flumazenil PET (Schmid *et al*, 1996; Bottlaender *et al*, 1997) and [123I]iomazenil SPECT (Sybirska *et al*, 1993). These studies, performed in anesthetized baboons,

measured the occupancy of the agonist drugs, such as diazepam and lorazepam, before and after alterations in endogenous GABA levels. Two studies by the same group noted the increased diazepam occupancy after increasing GABA with GVG pretreatment (Schmid *et al*, 1996) and decreased binding of diazepam after pretreatment with an inhibitor of GABA synthesis, DL-allylglycine (Bottlaender *et al*, 1997), findings consistent with the GABA-shift hypothesis. On the other hand, Sybirska *et al* (Sybirska *et al*, 1993) did not observe any increase in lorazepam binding after the administration of tiagabine, possibly due to the confounding effects of the anesthesia.

The strengths of this study include the measurement of the arterial input function, allowing for the assessment of the effects of tiagabine on V_{ND}, f_P and f_{ND}. While the absence of change in these variables post-tiagabine validates the use of either BP_P or BP_{ND} as an outcome measure, we chose to use BP_{ND}, derived through SRTM, as our primary outcome measure. Recent work has indicated that [11C]flumazenil is a substrate for p-glycoprotein (PGP), the major efflux pump in the blood–brain barrier (Ishiwata *et al*, 2007). Given this, we were concerned with the possibility that tiagabine may impact on the PGP, potentially altering brain delivery of [11C]flumazenil. The lack of difference in pons V_T indicates that this was not the case, however, it seemed prudent to use the SRTM for the analysis as, assuming PGP effects are uniform across brain regions, this methodology will result in BP_{ND} estimates, which are minimally affected by alterations in PGP function (Liow *et al*, 2007).

The relatively high variability in the percent change of [11C]flumazenil binding across subjects suggests that detecting differences between individuals with a psychiatric disorder and healthy controls may be challenging. However, variability in this range has been observed in other PET studies, which used a pharmacologic challenge to measure changes in neurotransmitter levels and have been able to detect between-group differences (Abi-Dargham *et al*, 2000; Martinez *et al*, 2007). A factor involved in this variability may be the timing of the PET scan relative to the administration of tiagabine. In this preliminary study, we attempted to time the PET scan such that scanning coincided with the reported T_{max} of the plasma concentration of tiagabine (45–60 min) to ensure the measurement occurred during the acute increase in GABA; however, review of microdialysis studies indicates GABA increases are sustained for several hours after oral administration of tiagabine. Although it is not known whether the GABA shift response will diminish within that time, for future studies, we intend to increase the time between tiagabine administration and scanning, allowing for more consistent absorption of tiagabine across subjects.

This extends the published literature with regards to the GABA shift, providing additional evidence supporting the idea that this phenomenon can be observed *in vivo*, using PET in humans. The ability to measure *in vivo* fluctuations in GABA levels provides a unique opportunity to explore the role of GABA in certain brain processes. Studies with nonhuman primates demonstrate that the disruption of GABA transmission in the DLFPC impairs working memory (Rao *et al*, 2000). In humans, DLPFC γ oscillations normally increase with working memory load (Howard *et al*, 2003), a phenomena, which is impaired in subjects with working memory deficits (Cho *et al*, 2006). In addition to playing a role in working memory (Howard *et al*, 2003), γ synchrony appears to be associated with other higher cognitive processes such as associative learning (Miltner *et al*, 1999). Although the specific role of GABA transmission in working memory is still under investigation, the synchronization of pyramidal cell firing by networks of fast-spiking, parvalbumin-containing GABA neurons gives rise to oscillatory activity in the γ range (Whittington and Traub, 2003). The strong relationship observed in this study between the change in [11C]flumazenil binding and the ability to entrain oscillatory activity in the γ frequency during a cognitive control task provides the first direct support for the hypothesis that GABA neurotransmission is linked to the synchronization of cortical neuronal activity in humans. The refinement and validation of the PET methodology described in this study would provide a unique ability to measure the changes in GABA levels *in vivo*; to examine the relationship between GABA neurotransmission, oscillatory activity, and cognition; and to explore the differences between control and patient populations in the degree of GABA increase in response to a standardized level of GAT1 blockade. Moreover, if abnormalities in GABA transmission exist in specific psychiatric disorders, this technique could be employed in the process of developing new pharmacologic compounds with the target of increasing cortical GABA levels.

ACKNOWLEDGEMENTS

We are grateful to the research subjects who participated in this study. We would like to thank Larry Kegeles, MD, for his input and expertize in designing and carrying out this study. We thank members of the PET Facility who carried out the acquisition of PET data and care of all subjects during PET procedures. These data were generated with the support of an NIH career development award (PI: Frankle), a Silvio O Conte Center for the Neuroscience of Mental Disorders (MH51456, PI: Lewis), and an NIH/NCRR grant, which funds the Montefiore University Hospital Clinical and Translational Research Center.

DISCLOSURES/CONFLICT OF INTEREST

The authors have no conflict of interest as it relates to the subject of this report.

- Dr Frankle receives speaking fees from Bristol Myers Squibb Inc., serves as a consultant for Sepracor Inc., Transcept Pharmaceuticals (formerly Transoral), and Eli Lilly Inc. He has received grant support from GlaxoSmith Kline Inc. and Sepracor Inc.
- Dr Narendran has received grant support from Glaxo-SmithKline Inc.
- Dr Mason serves as a consultant for NST Inc., Banner Good Samaritan Hospital (Phoenix, AZ), and The Gollman Group (Dallas, TX).
- Dr Price has received speaker fees from Servier.
- Dr Lewis currently receives research support from the BMS Foundation, Merck and Pfizer and in 2006–2008, served as a consultant to Bristol-Myers Squibb,

Hoffman-Roche, Lilly, Merck, Neurogen, Pfizer, Sepracor, and Wyeth.

- Dr Mathis receives royalty payments from the University of Pittsburgh for technology licensed to GE Healthcare and Neuroptix. He serves as a consultant for Elan, Pfizer, Takeda, Amgen, Baxter Scientific, Novartis, and GE Healthcare. He has received grant support from Neuroptix and GE Healthcare.

REFERENCES

Abadie P, Baron JC, Bisserbe JC, Boulenger JP, Rioux P, Travere JM *et al* (1992). Central benzodiazepine receptors in human brain: estimation of regional B_{max} and KD values with positron emission tomography. *Eur J Pharmacol* **213**: 107–115.

Abi-Dargham A, Laruelle M, Seibyl J, Rattner Z, Baldwin RM, Zoghbi SS *et al* (1994). SPECT measurement of benzodiazepine receptors in human brain with [123-I]iomazenil: kinetic and equilibrium paradigms. *J Nucl Med* **35**: 228–238.

Abi-Dargham A, Rodenhiser J, Printz D, Zea-Ponce Y, Gil R, Kegeles LS *et al* (2000). From the cover: increased baseline occupancy of D2 receptors by dopamine in schizophrenia. *Proc Natl Acad Sci USA* **97**: 8104–8109.

Barre L, Debruyne D, Abadie P, Moulin M, Baron JC (1991). A comparison of methods for separation of [11C]Ro 15-1788 (flumazenil) from its metabolites in the blood of rabbits, baboons, and humans. *Appl Radiat Isot* **42**: 435–439.

Bartos M, Vida I, Jonas P (2007). Synaptic mechanisms of synchronized gamma oscillations in inhibitory interneuron networks. *Nat Rev Neurosci* **8**: 45–56.

Bertrand O, Perrin F, Pernier J (1985). A theoretical justification of the average reference in topographic evoked potential studies. *Electroencephalogr Clin Neurophysiol* **62**: 462–464.

Bottlaender M, Schmid L, Fuseau C, Fournier D, Brouillet E, Maziere M (1997). *In vivo* modulation of benzodiazepine receptor function after inhibition of endogenous gamma-aminobutyyric acid synthesis. *Eur J Pharmacol* **321**: 13–17.

Braestrup C, Schmiechen R, Neef G, Nielsen M, Petersen EN (1982). Interaction of convulsive ligands with benzodiazepine receptors. *Science* **216**: 1241–1243.

Brambilla P, Perez J, Barale F, Schettini G, Soares JC (2003). GABAergic dysfunction in mood disorders. *Mol Psychiatry* **8**: 721–737, 715.

Breier A, Su TP, Saunders R, Carson RE, Kolachana BS, de Bartolomeis A *et al* (1997). Schizophrenia is associated with elevated amphetamine-induced synaptic dopamine concentrations: evidence from a novel positron emission tomography method. *Proc Natl Acad Sci USA* **94**: 2569–2574.

Cho RY, Konecky RO, Carter CS (2006). Impairments in frontal cortical gamma synchrony and cognitive control in schizophrenia. *PNAS* **103**: 19878–19883.

During M, Mattson R, Scheyer R, Rask C, Pierce M, McKelvy J *et al* (1992). *The Effect of Tiagabine HCI on Extracellular GABA Levels in the Human Hippocampus*. Annual Meeting of the American Epilepsy Society: Seattle, Washington.

Duvernoy H (1991). *The Human Brain Surface, Three-Dimensional Sectional Anatomy and MRI*. Sringer-Verlag Wien: New York.

Fink-Jensen A, Suzdak PD, Swedberg MD, Judge ME, Hansen L, Nielsen PG (1992). The gamma-aminobutyric acid (GABA) uptake inhibitor, tiagabine, increases extracellular brain levels of GABA in awake rats. *Eur J Pharmacol* **220**: 197–201.

Fuchs EC, Zivkovic AR, Cunningham MO, Middleton S, Lebeau FE, Bannerman DM *et al* (2007). Recruitment of parvalbumin-positive interneurons determines hippocampal function and associated behavior. *Neuron* **53**: 591–604.

Gyulai FE, Mintun MA, Firestone LL (2001). Dose-dependent enhancement of *in vivo* GABA(A)-benzodiazepine receptor binding by isoflurane. *Anesthesiology* **95**: 585–593.

Hajos N, Palhalmi J, Mann EO, Nemeth B, Paulsen O, Freund TF (2004). Spike timing of distinct types of GABAergic interneuron during hippocampal gamma oscillations *in vitro*. *J Neurosci* **24**: 9127–9137.

Halldin C, Stone-Enlander S, Thorell J-L, Persson A, Sedvall G (1988). 11C Labeling of Ro 15-1788 in two different positions, and also 11C labeling of its main metabolite Ro 15-3890, for PET studies of benzodiazepine receptors. *Appl Radiat Isot* **39**: 993–997.

Hashimoto T, Bazmi H, Mirnics K, Wu Q, Sampson A, Lewis D (in press). Conserved regional patterns of GABA-related transcript expression in the neocortex of subjects with schizophrenia. *Am J Psychiatry* **165**: 479–489.

Howard MW, Rizzuto DS, Caplan JB, Madsen JR, Lisman J, Aschenbrenner-Scheibe R *et al* (2003). Gamma oscillations correlate with working memory load in humans. *Cereb Cortex* **13**: 1369–1374.

Impagnatiello F, Guidotti AR, Pesold C, Dwivedi Y, Caruncho H, Pisu MG *et al* (1998). A decrease of reelin expression as a putative vulnerability factor in schizophrenia. *Proc Natl Acad Sci USA* **95**: 15718–15723.

Innis RB, Cunningham VJ, Delforge J, Fujita M, Gjedde A, Gunn RN *et al* (2007). Consensus nomenclature for *in vivo* imaging of reversibly binding radioligands. *J Cereb Blood Flow Metab* **27**: 1533–1539.

Ishiwata K, Kawamura K, Yanai K, Hendrikse NH (2007). *In vivo* evaluation of P-glycoprotein modulation of 8 PET radioligands used clinically. *J Nucl Med* **48**: 81–87.

Johannessen CU (2000). Mechanisms of action of valproate: a commentatory. *Neurochem Int* **37**: 103–110.

Klumpers UM, Veltman DJ, Boellaard R, Comans EF, Zuketto C, Yaqub M *et al* (2007). Comparison of plasma input and reference tissue models for analysing [(11)C]flumazenil studies. *J Cereb Blood Flow Metab* **28**: 579–587.

Koe BK, Kondratas E, Russo LL (1987). [^{3}H]Ro 15-1788 binding to benzodiazepine receptors in mouse brain *in vivo*: marked enhancement by GABA agonists and other CNS drugs. *Eur J Pharmacol* **142**: 373–384.

Koeppe RA, Holthoff VA, Frey KA, Kilbourn MR, Kuhl DE (1991). Compartmental analysis of [^{11}C]flumazenil kinetics for the estimation of ligand transport rate and receptor distribution using positron emission tomography. *J Cereb Blood Flow Metab* **11**: 735–744.

Konopaske GT, Sweet RA, Wu Q, Sampson A, Lewis DA (2006). Regional specificity of chandelier neuron axon terminal alterations in schizophrenia. *Neuroscience* **138**: 189–196.

Krystal JH, Staley J, Mason G, Petrakis IL, Kaufman J, Harris RA *et al* (2006). Gamma-aminobutyric acid type A receptors and alcoholism: intoxication, dependence, vulnerability, and treatment. *Arch Gen Psychiatry* **63**: 957–968.

Lammertsma AA, Hume SP (1996). Simplified reference tissue model for PET receptor studies. *Neuroimage* **4**: 153–158.

Laruelle M (2000). Imaging synaptic neurotransmission with *in vivo* binding competition techniques: a critical review. *J Cereb Blood Flow Metab* **20**: 423–451.

Laruelle M, Abi-Dargham A, van Dyck CH, Gil R, D'Souza CD, Erdos J *et al* (1996). Single photon emission computerized tomography imaging of amphetamine-induced dopamine release in drug-free schizophrenic subjects. *Proc Natl Acad Sci USA* **93**: 9235–9240.

Laruelle M, Baldwin RM, Rattner Z, Al-Tikriti MS, Zea-Ponce Y, Zoghbi SS *et al* (1994). SPECT quantification of [123I]iomazenil binding to benzodiazepine receptors in nonhuman primates. I. Kinetic modeling of single bolus experiments. *J Cereb Blood Flow Metab* **14**: 439–452.

Levenberg K (1944). A method for the solution of certain problems in least squares. *Quart Appl Math* **2**: 164–168.
Lewis DA, Hashimoto T, Volk DW (2005). Cortical inhibitory neurons and schizophrenia. *Nat Rev Neurosci* **6**: 312–324.
Liow JS, Lu S, McCarron JA, Hong J, Musachio JL, Pike VW *et al* (2007). Effect of a P-glycoprotein inhibitor, Cyclosporin A, on the disposition in rodent brain and blood of the 5-HT1A receptor radioligand, [11C](R)-(−)-RWAY. *Synapse* **61**: 96–105.
Lutzenberger W, Pulvermuller F, Elbert T, Birbaumer N (1995). Visual stimulation alters local 40-Hz responses in humans: an EEG study. *Neurosci Lett* **183**: 39–42.
Mann EO, Suckling JM, Hajos N, Greenfield SA, Paulsen O (2005). Perisomatic feedback inhibition underlies cholinergically induced fast network oscillations in the rat hippocampus *in vitro*. *Neuron* **45**: 105–117.
Martinez D, Gil R, Slifstein M, Hwang DR, Huang Y, Perez A *et al* (2005). Alcohol dependence is associated with blunted dopamine transmission in the ventral striatum. *Biol Psychiatry* **58**: 779–786.
Martinez D, Narendran R, Foltin RW, Slifstein M, Hwang DR, Broft A *et al* (2007). Amphetamine-induced dopamine release: markedly blunted in cocaine dependence and predictive of the choice to self-administer cocaine. *Am J Psychiatry* **164**: 622–629.
Miller LG, Greenblatt DJ, Barnhill JG, Summer WR, Shader RI (1988). 'GABA shift' *in vivo*: enhancement of benzodiazepine binding *in vivo* by modulation of endogenous GABA. *Eur J Pharmacol* **148**: 123–130.
Miltner WHR, Braun C, Arnold M, Witte H, Taub E (1999). Coherence of gamma-band EEG activity as a basis for associative learning. *Nature* **397**: 434–436.
Mintun MA, Raichle ME, Kilbourn MR, Wooten GF, Welch MJ (1984). A quantitative model for the *in vivo* assessment of drug binding sites with positron emission tomography. *Ann Neurol* **15**: 217–227.
Mohler H, Richards JG (1981). Agonist and antagonist benzodiazepine receptor interaction *in vitro*. *Nature* **294**: 763–765.
Nemeroff CB (2003). The role of GABA in the pathophysiology and treatment of anxiety disorders. *Psychopharmacol Bull* **37**: 133–146.
Persson A, Ehrin E, Eriksson L, Farde L, Hedstrom CG, Litton JE *et al* (1985). Imaging of [11C]-labelled Ro 15-1788 binding to benzodiazepine receptors in the human brain by positron emission tomography. *J Psychiatr Res* **19**: 609–622.
Price JC, Mayberg HS, Dannals RF, Wilson AA, Ravert HT, Sadzot B *et al* (1993). Measurement of benzodiazepine receptor number and affinity in humans using tracer kinetic modeling, positron emission tomography, and [^{11}C]-flumazenil. *J Cereb Blood Flow Metab* **13**: 656–667.
Rao SG, Williams GV, Goldman-Rakic PS (2000). Destruction and creation of spatial tuning by disinhibition: GABA (A) blockade of prefrontal cortical neurons engaged by working memory. *J Neurosci* **20**: 485–494.
Rosenberg HC, Chiu TH (1979). Benzodiazepine binding after *in vivo* elevation of GABA. *Neurosci Lett* **15**: 277–281.
Salmi E, Kaisti KK, Metsahonkala L, Oikonen V, Aalto S, Nagren K *et al* (2004). Sevoflurane and propofol increase 11C-flumazenil binding to gamma-aminobutyric acidA receptors in humans. *Anesth Analg* **99**: 1420–1426; table of contents.
Salmi E, Langsjo JW, Aalto S, Nagren K, Metsahonkala L, Kaisti KK *et al* (2005). Subanesthetic ketamine does not affect 11C-flumazenil binding in humans. *Anesth Analg* **101**: 722–725, table of contents.
Sanes J, Donoghue J (1993). Oscillations in local field potentials of the primate motor cortex during voluntary movement. *PNAS* **90**: 4470–4474.
Schmid L, Bottlaender M, Brouillet E, Fuseau C, Maziere M (1996). Vigabatrin modulates benzodiazepine receptor activity *in vivo*: a positron emission tomography study in baboon. *J Pharmacol Exp Ther* **276**: 977–983.
Smith SM, Jenkinson M, Woolrich MW, Beckmann CF, Behrens TE, Johansen-Berg H *et al* (2004). Advances in functional and structural MR image analysis and implementation as FSL. *Neuroimage* **23**(Suppl 1): S208–S219.
Sybirska E, Seibyl JP, Bremner JD, Baldwin RM, al-Tikriti MS, Bradberry C *et al* (1993). [123I]iomazenil SPECT imaging demonstrates significant benzodiazepine receptor reserve in human and nonhuman primate brain. *Neuropharmacology* **32**: 671–680.
Talairach J, Tournoux P (1988). *Co-Planar Stereotactic Atlas of the Human Brain. Three-Dimensional Proportional System: An Approach of Cerebral Imaging*. Theime Medical Publisher: New York.
Tallman JF, Thomas JW, Gallager DW (1978). GABAergic modulation of benzodiazepine binding site sensitivity. *Nature* **274**: 383–385.
Tiitinen H, Sinkkonen J, Reinikainen K, Alho K, Lavikainen J, Näätänen R *et al* (1993). Selective attention enhances the auditory 40-Hz transient response in humans. *Nature* **364**: 59–60.
Van Vreeswijk C, Abbott LF, Ermentrout GB (1994). When inhibition not excitation synchronizes neural firing. *J Comput Neurosci* **1**: 313–321.
Volkow ND, Wang GJ, Fowler JS, Logan J, Gatley SJ, Hitzemann R *et al* (1997). Decreased striatal dopaminergic responsiveness in detoxified cocaine-dependent subjects. *Nature* **386**: 830–833.
Watson C (2000). New, faster, image-based scatter correction for 3D PET. *IEEE Trans Nucl Sci* **47**: 1587–1594.
Weber OM, Verhagen A, Duc CO, Meier D, Leenders KL, Boesiger P (1999). Effects of vigabatrin intake on brain GABA activity as monitored by spectrally edited magnetic resonance spectroscopy and positron emission tomography. *Magn Reson Imaging* **17**: 417–425.
Whittington MA, Traub RD (2003). Interneuron diversity series: inhibitory interneurons and network oscillations *in vitro*. *Trends Neurosci* **26**: 676–682.
Woo TU, Walsh JP, Benes FM (2004). Density of glutamic acid decarboxylase 67 messenger RNA-containing neurons that express the N-methyl-D-aspartate receptor subunit NR2A in the anterior cingulate cortex in schizophrenia and bipolar disorder. *Arch Gen Psychiatry* **61**: 649–657.
Zhang Y, Brady M, Smith S (2001). Segmentation of brain MR images through a hidden Markov random field model and the expectation-maximization algorithm. *IEEE Trans Med Imaging* **20**: 45–57.